Neuroimaging-Based Assessments of OXPHOS-Related Complexes and Metabolites

Subjects: Anatomy & Morphology

Contributor: Jannik Prasuhn , Liesa Kunert , Norbert Brüggemann

In post-mortem studies, a significant dysregulation of electron transport chain (ETC) complexes was observed in patients with neurodegenerative diseases (NDs). These findings strongly implicate that mitochondrial dysfunction-linked alterations in oxidative phosphorylation (OXPHOS) can be considered a highly relevant molecular mechanism in different NDs. Histopathological examinations revealed decreased complex I level, preferentially in the substantia nigra (SN), in patients suffering from Parkinson's disease (PD). These findings are consistent with the fact that inhibitors of complex I (such as the environmental toxins MPTP or rotenone) can cause parkinsonism in animal models and humans. Huntington's disease (HD) has been associated with defects of complex II and, to a lesser extent, complex IV. The chronic administration of the complex II inhibitor 3-nitropropionic acid causes an HD-like phenotype in rodent and non-human primate models. In Alzheimer's disease (AD), widespread cortical complex IV defects were identified in post-mortem brain tissue. The in vivo neuroimaging-based assessment of electron transport chain (ETC)-related metabolite levels could thus help elucidate the complex role of OXPHOS disturbances in NDs.

OXPHOS-Related Complexes and Metabolites Neuroimaging

1 . ^{31}Phosphorus-Magnetic Resonance Spectroscopy Imaging to Quantify Oxidative Phosphorylation (OXPHOS)-Related Metabolite Levels In Vivo

In general, magnetic resonance spectroscopy (MRSI) can provide a unique view into these metabolic processes in vivo [1]. Nuclear magnetic resonance (NMR)-active nuclei are partially shielded from the static magnetic field by surrounding electrons, which causes slight magnetic field distortions. These distortions result in so-called chemical shifts (usually expressed in parts per million, ppm), which can be used to identify distinct metabolites in a spectrum based on their known molecular structure [2]. Besides the flexibility and widespread applicability of ^{1}H-MRSI, ^{31}P-MRSI offers unique opportunities to investigate OXPHOS-related mitochondrial dysfunction in vivo. The ^{31}P nucleus has a significantly lower gyromagnetic ratio compared to ^{1}H. However, the natural abundance of the ^{31}P nucleus in living tissues is close to 100%, resulting in robust NMR signals [3]. Therefore, ^{31}P-MRSI can be applied to map high-energy phosphorus-containing metabolites (HEPs), such as adenosine triphosphate (ATP) or phosphocreatine (PCr), in vivo [3] (see **Figure 1**).

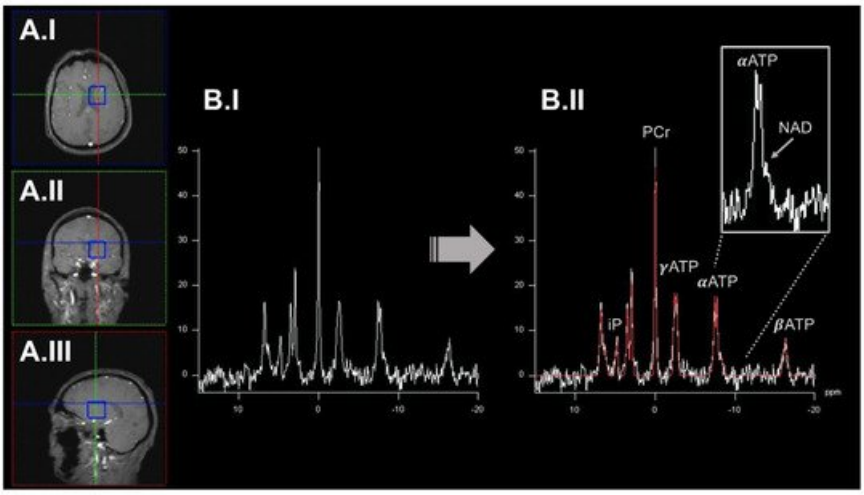

Figure 1. An exemplary illustration of ^{31}P-MRSI acquisition workflow. it was highlighted that an acquired spectrum from a single voxel (blue box) displayed in axial (panel (**A.I**)), coronal (panel (**A.II**)), and sagittal (panel (**A.III**)). The preprocessed (before peak-annotation) spectrum is shown in panel (**B.I**). In panel (**B.II**), the different peaks of the spectrum have been annotated based on a model fit (highlighted in red) by incorporating prior knowledge. Metabolite levels can be quantified by calculating the respective area under the peak. ATP gives rise to three signal peaks (α/β/γATP) based on the number of phosphorus nuclei in this molecule. Some metabolite peaks overlap (e.g., αATP and NAD; right upper corner). Here, elaborate experimental setups, acquisition protocols, and higher static magnetic field strengths are desirable to disentangle these metabolites. ^{31}P-MRSI: ^{31}phosphorus magnetic resonance spectroscopy imaging. ATP: adenosine triphosphate. iP: inorganic phosphate. NAD: nicotinamide adenine dinucleotide. PCr: phosphocreatinine. ppm: parts per million.

High-Energy Phosphorus (HEPs) can be interpreted as the end route of OXPHOS. In previous studies, HEPs have been expressed as a ratio to inorganic phosphate (iP) to account for intraindividual differences, e.g., in the alimentary intake of phosphorus-containing nutrients [4]. HEPs can form a highly dynamic equilibrium and can be considered together to describe the cerebral bioenergetic state. The in vivo concentrations of AMP and ADP are usually below the detection limits of ^{31}P-MRSI. In addition, the reliable quantification of AMP/ADP is hindered by the spectral overlap to other metabolites [3]. The in vivo study of HEPs has already been applied to patients with Parkinson's disease (PD) [5], atypical Parkinson's disease (APD) [6], Alzheimer's disease (AD) [4], and Huntington's disease (HD) [7], among others. In addition, NAD can also be quantified by ^{31}P-MRSI [8][9]. NAD is an essential coenzyme in various redox reactions and can be present in a reduced (NADH) or oxidized (NAD^+) state. NADH is the substrate of complex I of the ETC (the starting point of OXPHOS). In addition, experimental evidence suggests that the NADH/NAD^+ ratio plays a crucial role in regulating OXPHOS and maintaining overall mitochondrial homeostasis [10]. The NADH/NAD^+ ratio could be a surrogate marker of complex I activity and the general neuronal bioenergetic and redox state. Based on the substantial spectral overlap of NADH and NAD^+, the ^{31}P-MRSI-based differentiation of these metabolites requires elaborate experimental procedures. State-of-the-art ^{31}P-MRSI platforms have proven the technical feasibility of NAD^+/NADH differentiation in vivo [8][9]. Numerous studies have demonstrated the involvement of NAD metabolism in NDs, such as in AD or PD. Decreased NAD levels have been observed in both patient groups [10]. These findings finally led to the clinical evaluation of NAD precursors as potential treatments, e.g., for PD [11]. In general, MRSI studies benefit from high or ultrahigh magnetic field strengths to, e.g., shorten T1 relaxation times. Moreover, increased spectral resolution can substantially improve the differentiation of neighboring or partially overlapping peaks in ^{31}P-MRSI-derived spectra [2].

2. Dynamic Measurements of OXPHOS Reaction Kinetics by ^{31}phosphorus Magnetization Transfer Magnetic Resonance Spectroscopy Imaging

Combining ^{31}P-MRSI with magnetization transfer preparation pulses (^{31}P-MT-MRSI) can quantify OXPHOS-related kinetic reaction parameters of in vivo ATP metabolism [12]. In particular, three reaction rates have been the subject of previous research: iP ⇋ ATP, iP ⇋ PCr, and PCr ⇋ ATP [12]. Determining these steady-state reaction rates opens up many exciting opportunities to study brain energy metabolism in NDs in-depth. The ^{31}P-MT-MRSI methodology has already been used to study patients with HD [7]. After visual stimulation, an increase in iP ⇋ PCr and iP ⇋ ATP ratios was observed in the occipital lobe of these patients. Following a similar experimental procedure, the investigational nutritional supplement triheptanoin restored the iP ⇋ PCr ratio in early-stage HD patients by providing TCA cycle substrates [13]. ^{31}P-MT-MRSI can therefore be of particular interest to foster the understanding of impaired PCr metabolism, which has previously been implicated in HD [14]. However, the technical complexity of ^{31}P-MT-MRSI hinders its widespread applicability in NDs research. ^{31}P-MT-MRSI remains an active research area but has already been applied in other NDs, such as monogenic and idiopathic PD [5].

3. Quantitative Assessment of Mitochondrial Complex I by Positron Emission Tomography Imaging Radiotracer

Based on the prominent role of complex I disturbances in NDs, several PET radiotracers have been evaluated for quantitative imaging [15]. Out of these, the radiotracer ^{18}F-BCPP-EF has entered clinical evaluation. Rodent studies have shown that ^{18}F-BCPP-EF yields a high molecular specificity and undergoes dynamic changes following the administration of complex I inhibitors [16]. Studies in non-human primates additionally validated these findings in conscious, untreated, and MPTP-treated animals [17][18]. ^{18}F-BCPP-EF is currently under investigation for the assessment of patients with NDs. In PD patients, decreased binding levels of ^{18}F-BCPP-EF have been observed in several neuroanatomical key structures without reaching statistical significance [19]. In the same study, the longitudinal assessment of PD patients showed a trend without reaching the significance level [19]. In a multimodal PET imaging study in patients with AD, ^{18}F-BCPP-EF binding is closely associated with the in vivo tau deposition but not the overall amyloid load [20]. ^{18}F-BCPP-EF yields immense promises for evaluating mitochondrial dysfunction in patients with NDs. Even though more extensive studies are needed to assess the clinical applicability, a recent study has shown a convincingly high test-retest variability as an essential prerequisite for upcoming clinical trials [21].

4. Broadband Near-Infrared Spectroscopy to Dynamically Map Cytochrome c Oxidase Activity

NIRS helps to understand in vivo brain physiology and disease states non-invasively. Near-infrared light can, to a certain extent, penetrate living tissues. Here, absorbent molecules (so-called chromophores) can be measured by their respective tissue-related light attenuation [22]. Neuroscientists have widely used NIRS to measure changes in oxygenated (HbO_2) and deoxygenated (Hb) hemoglobin, mainly following neuronal activation. Here, distinct frequencies of the near-infrared spectrum are usually used to map HbO_2/Hb [22]. The mitochondrial enzyme cytochrome c oxidase (CCO) is one of the most abundant enzymes found in mammals. CCO can also serve as a chromophore in NIRS studies. Interestingly, the extinction spectrum of CCO changes based on its respective redox state (CCO vs. oxCCO) [23]. This phenomenon is of particular interest to measure OXPHOS disturbances by this methodology. However, lower CCO concentrations compared to HbO_2/Hb chromophores pose a significant challenge for standard NIRS techniques [23]. CCO shows a broad absorption peak that is significantly different from HbO_2/Hb chromophores [22]. Specific hardware setups are needed to disentangle the signals

derived from the other chromophores in vivo. Ongoing advancements in standard NIRS technology led to the development of a method called broadband NIRS (bNIRS) [23]. bNIRS emits light within a wide frequency-range of the near-infrared spectrum to overcome these challenges [23]. Several in vitro and in vivo studies have demonstrated the successful separation of the CCO/oxCCO signal from HbO_2/Hb changes by bNIRS [22]. Usually, physiological challenges are required to induce CCO/oxCCO signal changes. Within the given experimental setup, physiological parameters (e.g., the breathing rate) must be carefully monitored and considered as potential cofounders of derived findings [24][25]. The overall interpretation of derived CCO/oxCCO signal changes can be assisted by physiological models already available [26]. Unfortunately, these devices are currently not commercially available. In addition, many experimental options are available, including different algorithms for data processing, the precise definition of chromophore absorption spectra, and the number and variety of emitted wavelengths.

Abbreviations

(b)NIRS: (broadband) near-infrared spectroscopy imaging. (ox)CCO: oxidized cytochrome c oxidase. ^{18}F-BCPP-EF: 2-tert-butyl-4-chloro-5-(6-(2-(2(18F)fluoroethoxy) -ethoxy]-pyridin-3-ylmethoxy)-2H-pyridazin-3-one. AD: Alzheimer's disease. ADP: adenosine diphosphate. AMP: adenosine monophosphate. APD: atypical parkinsonism. ASL: arterial spin labeling. ATP: adenosine triphosphate. DNA: deoxyribonucleic acid. ETC: electron transport chain. HD: Huntington's disease. HEP: high-energy phosphorus-containing metabolites. iP: inorganic phosphate. MND: motor neuron disease. MPTP: 1-methyl-4-phenyl-1,2,3,6-tetrahydropyridine. MRI: magnetic resonance imaging. MRSI: magnetic resonance spectroscopy imaging. MT-MRSI: magnetization transfer magnetic resonance spectroscopy imaging. mtDNA: mitochondrial DNA. NAD/NAD+/NADH: nicotinamide adenine dinucleotide. ND: neurodegenerative diseases. NMR: nuclear magnetic resonance. OEF: oxygen extraction fraction. OXPHOS: oxidative phosphorylation. PD: Parkinson's disease. PET: positron emission tomography. QUEST-MRI: QUEnch-assiSTed-MRI. ROS: reactive oxygen species. SN: substantia nigra. SNR: signal-to-noise ratio. TCA: tricarboxylic acid.

References

1. Zhu, X.H.; Lu, M.; Chen, W. Quantitative imaging of brain energy metabolisms and neuroenergetics using in vivo X-nuclear 2H, 17O and 31P MRS at ultra-high field. J. Magn. Reson. 2018, 292, 155–170.
2. Buonocore, M.H.; Maddock, R.J. Magnetic resonance spectroscopy of the brain: A review of physical principles and technical methods. Rev. Neurosci. 2015, 26, 609–632.
3. Liu, Y.; Gu, Y.; Yu, X. Assessing tissue metabolism by phosphorous-31 magnetic resonance spectroscopy and imaging: A methodology review. Quant. Imaging Med. Surg. 2017, 7, 707–726.
4. Das, N.; Ren, J.; Spence, J.; Chapman, S.B. Phosphate Brain Energy Metabolism and Cognition in Alzheimer's Disease: A Spectroscopy Study Using Whole-Brain Volume-Coil 31Phosphorus Magnetic Resonance Spectroscopy at 7Tesla. Front. Neurosci. 2021, 15, 641739.
5. Rango, M.; Dossi, G.; Squarcina, L.; Bonifati, C. Brain mitochondrial impairment in early-onset Parkinson's disease with or without PINK1 mutation. Mov. Disord. 2020, 35, 504–507.
6. Stamelou, M.; Pilatus, U.; Reuss, A.; Magerkurth, J.; Eggert, K.M.; Knake, S.; Ruberg, M.; Schade-Brittinger, C.; Oertel, W.H.; Hoglinger, G.U. In vivo evidence for cerebral depletion in high-energy phosphates in progressive supranuclear palsy. J. Cereb. Blood Flow Metab. 2009, 29, 861–870.
7. Mochel, F.; N'Guyen, T.M.; Deelchand, D.; Rinaldi, D.; Valabregue, R.; Wary, C.; Carlier, P.G.; Durr, A.; Henry, P.G. Abnormal response to cortical activation in early stages of Huntington disease.

Mov. Disord. 2012, 27, 907–910.

8. Lu, M.; Zhu, X.H.; Zhang, Y.; Chen, W. Intracellular redox state revealed by in vivo (31) P MRS m easurement of NAD(+) and NADH contents in brains. Magn. Reson. Med. 2014, 71, 1959–1972.
9. Lu, M.; Zhu, X.H.; Chen, W. In vivo (31) P MRS assessment of intracellular NAD metabolites and NAD(+) /NADH redox state in human brain at 4 T. NMR Biomed. 2016, 29, 1010–1017.
10. Reiten, O.K.; Wilvang, M.A.; Mitchell, S.J.; Hu, Z.; Fang, E.F. Preclinical and clinical evidence of NA D(+) precursors in health, disease, and ageing. Mech. Ageing Dev. 2021, 199, 111567.
11. Chong, R.; Wakade, C.; Seamon, M.; Giri, B.; Morgan, J.; Purohit, S. Niacin Enhancement for Parki nson's Disease: An Effectiveness Trial. Front. Aging Neurosci. 2021, 13, 667032.
12. Du, F.; Zhu, X.H.; Qiao, H.; Zhang, X.; Chen, W. Efficient in vivo 31P magnetization transfer appr oach for noninvasively determining multiple kinetic parameters and metabolic fluxes of ATP met abolism in the human brain. Magn. Reson. Med. 2007, 57, 103–114.
13. Adanyeguh, I.M.; Rinaldi, D.; Henry, P.G.; Caillet, S.; Valabregue, R.; Durr, A.; Mochel, F. Trihepta noin improves brain energy metabolism in patients with Huntington disease. Neurology 2015, 8 4, 490–495.
14. van den Bogaard, S.J.; Dumas, E.M.; Teeuwisse, W.M.; Kan, H.E.; Webb, A.; van Buchem, M.A.; Ro os, R.A.; van der Grond, J. Longitudinal metabolite changes in Huntington's disease during disea se onset. J. Huntingtons Dis. 2014, 3, 377–386.
15. Harada, N.; Nishiyama, S.; Kanazawa, M.; Tsukada, H. Development of novel PET probes, BCPP-E F, BCPP-BF, and BCPP-EM for mitochondrial complex 1 imaging in the living brain. J. Labelled Co mp. Radiopharm. 2013, 56, 553–561.
16. Tsukada, H.; Nishiyama, S.; Fukumoto, D.; Kanazawa, M.; Harada, N. Novel PET probes 18F-BCPP -EF and 18F-BCPP-BF for mitochondrial complex I: A PET study in comparison with 18F-BMS-747 158-02 in rat brain. J. Nucl. Med. 2014, 55, 473–480.
17. Tsukada, H.; Ohba, H.; Kanazawa, M.; Kakiuchi, T.; Harada, N. Evaluation of 18F-BCPP-EF for mito chondrial complex 1 imaging in the brain of conscious monkeys using PET. Eur. J. Nucl. Med. Mol. Imaging 2014, 41, 755–763.
18. Tsukada, H.; Kanazawa, M.; Ohba, H.; Nishiyama, S.; Harada, N.; Kakiuchi, T. PET Imaging of Mito chondrial Complex I with 18F-BCPP-EF in the Brains of MPTP-Treated Monkeys. J. Nucl. Med. 2016, 57, 950–953.
19. Wilson, H.; Pagano, G.; de Natale, E.R.; Mansur, A.; Caminiti, S.P.; Polychronis, S.; Middleton, L.T.; Price, G.; Schmidt, K.F.; Gunn, R.N.; et al. Mitochondrial Complex 1, Sigma 1, and Synaptic Vesicl e 2A in Early Drug-Naive Parkinson's Disease. Mov. Disord. 2020, 35, 1416–1427.
20. Terada, T.; Therriault, J.; Kang, M.S.P.; Savard, M.; Pascoal, T.A.; Lussier, F.; Tissot, C.; Wang, Y.T.; Benedet, A.; Matsudaira, T.; et al. Mitochondrial complex I abnormalities is associated with tau a nd clinical symptoms in mild Alzheimer's disease. Mol. Neurodegener. 2021, 16, 28.
21. Mansur, A.; Rabiner, E.A.; Tsukada, H.; Comley, R.A.; Lewis, Y.; Huiban, M.; Passchier, J.; Gunn, R. N. Test-retest variability and reference region-based quantification of (18)F-BCPP-EF for imaging mitochondrial complex I in the human brain. J. Cereb. Blood Flow Metab. 2021, 41, 771–779.
22. Bale, G.; Elwell, C.E.; Tachtsidis, I. From Jobsis to the present day: A review of clinical near-infrar ed spectroscopy measurements of cerebral cytochrome-c-oxidase. J. Biomed. Opt. 2016, 21, 09 1307.
23. Lange, F.; Dunne, L.; Hale, L.; Tachtsidis, I. MAESTROS: A Multiwavelength Time-Domain NIRS Sy stem to Monitor Changes in Oxygenation and Oxidation State of Cytochrome-C-Oxidase. IEEE J. Sel. Top. Quantum Electron. 2019, 25, 7100312.
24. Kovacsova, Z.; Bale, G.; Mitra, S.; de Roever, I.; Meek, J.; Robertson, N.; Tachtsidis, I. Investigatio n of Confounding Factors in Measuring Tissue Saturation with NIRS Spatially Resolved Spectrosc

opy. Adv. Exp. Med. Biol. 2018, 1072, 307–312.

25. Caldwell, M.; Scholkmann, F.; Wolf, U.; Wolf, M.; Elwell, C.; Tachtsidis, I. Modelling confounding effects from extracerebral contamination and systemic factors on functional near-infrared spectroscopy. Neuroimage 2016, 143, 91–105.
26. Russell-Buckland, J.; Kaynezhad, P.; Mitra, S.; Bale, G.; Bauer, C.; Lingam, I.; Meehan, C.; Avdic-Belltheus, A.; Martinello, K.; Bainbridge, A.; et al. Systems Biology Model of Cerebral Oxygen Delivery and Metabolism During Therapeutic Hypothermia: Application to the Piglet Model. Adv. Exp. Med. Biol. 2021, 1269, 31–38.